Scientific Programs and Required Beamline Performance at LiX

Noncrystalline biological samples often exhibit various levels of structural complexity that produce scattering signal within a wide range of scattering angles, or q values. q is the scattering vector defined as $q = \frac{4\pi}{\lambda}\sin\theta$, where λ is the x-ray wavelength and 2θ is the scattering angle. These samples are also often weak x-ray scatterers, due to the low electron density contrast. X-ray measurements on these samples therefore require high x-ray intensity as well as low x-ray divergence. Taking advantage of the NSLS-II source brightness, the LIX beamline will provide capabilities for transmission and grazing incidence x-ray scattering with tunable beam size and divergence, to support scientific research in three specific areas: 1) structural dynamics of biological molecules in solution on a time scale of tens of microseconds to sub-seconds, 2) structure characterization of planar lipid membranes and the associated membrane proteins, and 3) x-ray scattering-based scanning probe mapping at micron resolution of organic and inorganic matrices in biological tissues.

1 Time-Resolved Scattering from Macromolecules and Complexes in Solution

1.1 Scientific Motivation

At the molecular level, biological processes involve the assembly of macromolecules into their functional forms and interactions between functional molecules. The former, self-assembly problem has attracted a great deal of interest in the scientific community with much attention paid to both protein and RNA folding. The motivation for studying folding is two-fold. On one hand, it is of fundamental interest to understand how molecules of a given linear amino acid or nucleotide sequence fold into their functional 3-dimensional structure and how this functional structure can be predicted. Because of the strong link between protein structure and function, much effort to date has been devoted to the study of protein folding[1–3]. For proteins, there has also been much effort devoted to misfolding because of the strong link with numerous human diseases[4]. Neurodegenerative diseases such as Alzheimer's, Parkinson's, Lou Gehrig's, and Huntington's disease have been linked to aggregation or a toxic gain of function for specific proteins or peptides. Protein misfolding has also been associated with cataracts, type II diabetes, and a multitude of amyloidoses[4,5].

To understand the molecular underpinnings of protein aggregation and/or toxicity, it is necessary to know the populations and structures of not just the most stable native state of the protein but also higher energy, less populated, partially folded structures[5]. These states, other potentially misfolded states, and oligomers of proteins have been hypothesized as the toxic species in a number of diseases and are the focus of an increasing body of current research[4,5]. It is expected that a greater understanding of their structure, dynamics, and thermodynamics is also likely to be a launching point in efforts toward finding therapeutics[6,7]. The ability to map and understand the energy landscape of proteins through both experimental and computational approaches is therefore of increasing significance to outstanding issues in biology and human disease. The structural and kinetic information obtained from time-resolved small-angle x-ray scattering (SAXS) meets a critical need in this regard.

RNA folding has recently emerged as an important problem, driven by the ongoing recognition of RNA's central roles in the cell. For example, RNA conformational dynamics are now recognized as control elements in gene expression[8]. These riboswitches can fold into two distinct structures: one that allows gene expression, another that prevents it. Furthermore, it has now been established[9] that significantly more RNA is *transcribed* than *translated;* in other words, much

more RNA is copied from DNA than the fraction that codes for proteins. The biological roles of these numerous molecules may become evident if their folded structures can be derived from sequence.

In a time-resolved mode, SAXS is expected to provide structural information on time scales as short as tens of microseconds. When coupled with recent advances in molecular dynamics simulations (see the folding@home distributed computing project at http://folding.stanford.edu/, for example), a convergence of experiment and simulation is imminent, resulting in an unprecedented synergy between the two in the biological sciences.

Folding of either proteins or RNA is a complex process with many sequential (or parallel) events occurring over a wide range of time scales. Folding has been investigated with various techniques (**Figure 1**). X-ray scattering is a particularly valuable tool for monitoring the overall size and shape of these macromolecules as they fold. SAXS studies of the earliest folding events provide unique information about the structures of the non-native states that form within microseconds of the initiation of the folding reaction. These states can be "invisible" to other structural probes, notably those sensitive to the presence of structural contacts or those in which the states are obscured by dynamical averaging.

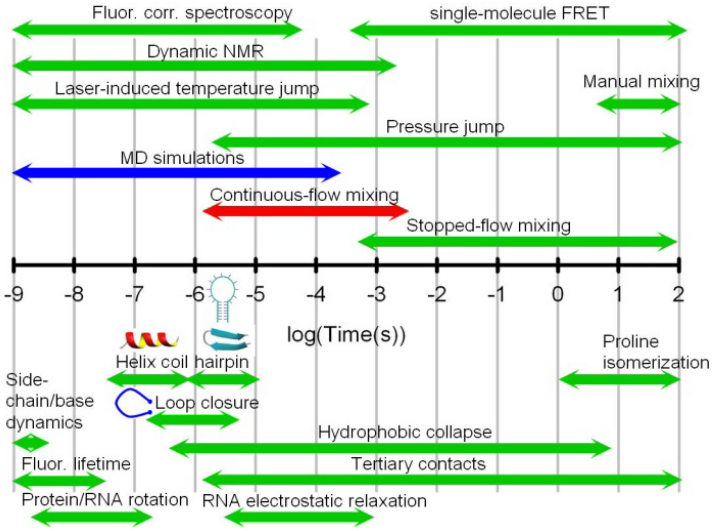

Figure 1. Time scales involved in folding events and the technique that can be applied to folding studies.

While protein and RNA folding have been the most visible application, time-resolved solution scattering can also be used to study other dynamic processes such as protein conformation change triggered by ligand-binding or enzymatic reaction. The characteristic time scales in these processes are likely to be milliseconds or slower; therefore these measurements are not as technically challenging as the folding measurements. However, applications of time-resolved solution scattering in this research area will likely see major growth, in academic research as well as in industrial drug development. For instance, there is a major effort to search for glucokinase activators (GKAs) for diabetes treatment[10]. Glucokinase (GK) catalyzes the first and rate-limiting step in converting glucose to glycogen for storage. It stimulates insulin secretion in β-cells and enhances glucose uptake in the liver. It is the only known monomeric protein shown to have positive cooperativity with its substrate, glucose, which is critical for its glucose-sensing role. Inactivating GK mutations causes diabetes, and activating mutations causes persistent hyperinsulinemic hypoglycemia, underscoring the importance of GK. Small-molecule GK activators are proven effective in treating diabetes in clinical trials, but hypoglycemia is a major safety risk, resulting in two major pharmaceutical companies terminating their GKA programs. Time-resolved scattering studies of the interaction between GK, glucose, and GKA will improve

the understanding of GK kinetics and activation, and how GKAs affect its kinetics, thereby providing guidance for the design of better and safer GKAs.

1.2 Technical Requirements

Time-resolved SAXS measurements at time scales from tens of microseconds to hundreds of milliseconds will require a combination of continuous and stopped flow mixers[11,12]. In these devices, conformation changes in the macromolecule are triggered by rapidly introducing its ligands or reaction partners into the vicinity of the macromolecule via rapid diffusion across short length scales.

Continuous flow mixing. Both laminar flow mixing[13] and turbulent mixing[14] have been successfully employed to probe reactions on the sub-millisecond time scale. In these continuous flow mixers, molecular conformation is monitored as a function of distance along a detection channel, which corresponds to time after mixing. The flow speed is the scale factor that converts position along the channel into reaction time. Since the beam remains 'parked' at one place while the sample flows by, exposure times can be as long as minutes with no concern about radiation damage. Thus, sharp time resolution is enabled with good signal-to-noise ratio (SNR). The brightness of the NSLS-II undulator source is therefore ideal for these measurements because small beam sizes can be obtained without compromising the low beam divergence that is required for high-quality SAXS measurements.

Two different mixing strategies have been employed to date. Turbulent mixers (**Figure 2**A) will likely provide the best time resolution in x-ray scattering measurements.

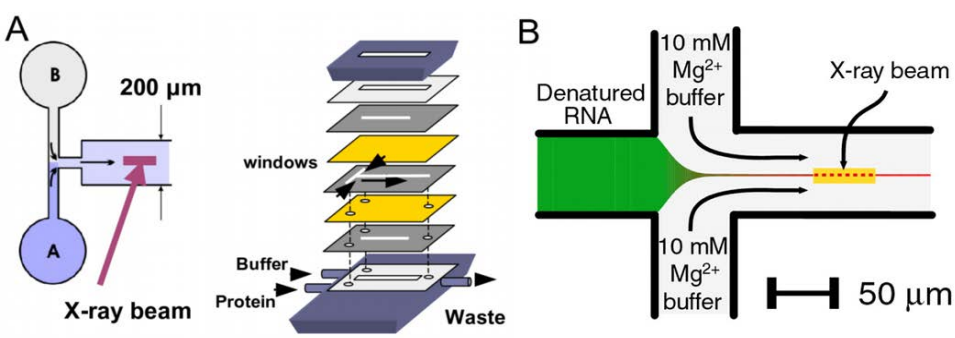

Figure 2. Schematic illustrations of continuous flow mixers. (A) A turbulent mixer[14] and (B) a laminar flow mixer[11]. In both cases, the time-scale probed is determined by the distance from the x-ray beam position to the onset of mixing. While the constructions of the two mixers are similar, turbulent flow dominates in (A); therefore the flow profile is uniform transverse to the beam. In contrast, in (B) the sample is confined within the thin jet at the center of the channel and occupies a much smaller volume.

In these devices, plug flow is achieved in the observation channel. Therefore, the time resolution is mainly limited by the mixing time. An arrowhead mixer has been demonstrated to achieve a mixing time of ~30 µs in fluorescence measurements using a tightly focused laser for excitation. However, in x-ray measurements, the larger beam size currently available necessitated modifications to the mixer design and limited the time resolution to ~200 µs[15,16]. The mixing time of this device can be improved to ~20 µs by using flow channel widths comparable to those used in fluorescence measurements[14], and additional optimization of the design can be achieved by introducing a serpentine pattern in the mixing region and asymmetric input channel widths. Some of these design improvements have been manufactured and are currently being tested. Such a mixer requires an x-ray beam size of ~50 µm (parallel to flow) x 20 µm (perpendicular to flow). Sample consumption is high for turbulent mixers because of the need to maintain a high flow rate and high Reynolds number. However, because the observation region is comparable in size to

static samples, the SNR and sample concentration requirements (~1 mg/mL) are also comparable to static measurements. Additionally, the possibility of radiation damage and heating of the samples by the x-ray beam is minimized, owing to the high flow rate.

At the other extreme, laminar flow mixers (**Figure 2**B) have been employed to study both RNA and protein folding with ~millisecond time resolution[13,17]. With next-generation design improvements[18] that focus on increasing mixing uniformity and eliminating parabolic flow profiles, the shortest time scale that can be probed in x-ray measurement with these mixers will likely be 10–100 microsec. While sharper time resolution has been reported for comparably designed mixers in optical spectroscopy studies, practical considerations for SAXS measurements require wider and deeper channels. Realistically, jet widths of about 1 µm flowing within devices that are about 1 mm deep (providing a good x-ray path length) can be used in conjunction with focused x-ray beam sizes of 10 µm (parallel to flow) x 5 µm (perpendicular to flow) or smaller. The great advantage of these mixers, however, is that sample consumption is minimized. Nearly every molecule that flows through the mixer will be sampled by the x-ray beam. We anticipate that access to time scales on the order of tens of microseconds will be relatively straightforward, opening up more than an order of magnitude in time resolution to SAXS studies of this type. One example of the new science that will be enabled in this regime is measurements of the initial collapse of RNA molecules. These measurements are critical for RNA since the "denatured" states of RNA likely bias the folding landscape[19–21].

Stopped flow mixing. To access time scales of milliseconds and longer, a stopped flow device can be used. These devices are commercially available and are being used at synchrotron beamlines around the world. The x-ray beam illuminates the sample within a short time window after stopped flow mixing is triggered. Multiple exposures can be collected after mixing within the limit of sample radiation damage. Commercial stopped flow devices usually employ a glass capillary as the sample cell in the observation chamber. A cell with flat windows[22] is more desirable, so that the x-ray beam size at the sample can be increased (e.g., to ~0.4 mm, as is often used for bulk samples at beamline X9) in order to reduce the average radiation dose deposited into the sample, thereby increasing the range of time scales that can be probed after each mixing event.

In all cases of time-resolved solution scattering, useful scattering data are expected within small scattering angles only, in the q-range of ~0.006–0.3 $Å^{-1}$. Measurements using the stopped flow device will be carried out at x-ray energies of 12 keV or above to minimize radiation damage to the samples. Anomalous scattering measurements at lower energies, e.g., near the K-edge of calcium near 4 keV, are possible using continuous flow mixers, where the sample exposed to the x-ray beam is constantly refreshed.

2 Two-Dimensional Membrane Structures

2.1 Scientific Motivation

Membrane proteins represent about one-third of the known gene sequences and are involved in various biological processes that take place at cell and organelle membranes, such as cell recognition, signal transduction, chemical sensing, and transportation. Defects in membrane proteins have been linked to various diseases. While the membrane proteins have attracted most attention in the studies of cellular processes that involve membranes, a complete understanding of these processes requires structural information on both the membrane proteins and the associated lipid bilayers. The bilayer may play a regulatory role, or even actively participate in the biological process, as in pore formation and membrane fusion. Currently there exist some limited examples of x-ray scattering and diffraction studies of lipid membranes. X-ray studies of membrane proteins have been largely limited to attempts to use solution scattering to study detergent-micelle

complexes. There is also no dedicated synchrotron radiation facility for biological membrane research at this time. NSLS-II provides a unique opportunity to develop new x-ray scattering methods for studying membrane structures.

The key difficulty that has limited the progress in x-ray scattering studies of membrane proteins is that they are not soluble in aqueous solutions. Therefore, traditional x-ray scattering and crystallography methods can only be used to study soluble membrane protein detergent complexes, which are membrane proteins extracted out of the membranes by detergent solubilization. However, the use of detergents often complicates the process of crystal growth. Even in cases where crystal structures have been obtained, the precise location and orientation of the membrane protein can only be inferred from the hydrophobic residues located on the surface of the membrane protein. Detergents could also distort the protein from its native conformation.

Membrane proteins can be incorporated into two-dimensional (2D) planar membranes that resemble their native environment in a liquid-like state. This sample configuration is a promising alternative for examining the structures of membrane proteins and how they interact with the lipid membrane. In these structures, the x-ray scattering signal is determined by the electron density contrast of the protein against the constant background of the bilayer membrane structure, which can be determined separately by x-ray reflectivity. The net electron density contrast not only depends on the structure of the protein itself, but also varies as a function of the location and orientation of the protein in the membrane. Electron density contrast is even sensitive to structural details such as the deformation of the membrane due to hydrophobic mismatching. It should be possible to determine these structural variables by comparing the experimental data with theoretical calculations based on the NMR/crystal structure or computational models of the membrane proteins.

The feasibility of this approach is demonstrated in **Figure 3** by the simulated scattering data from a single lipid bilayer that contains membrane protein zinc transporter YiiP[23,24], in its open and closed conformations, as shown in **Figure 3**A.

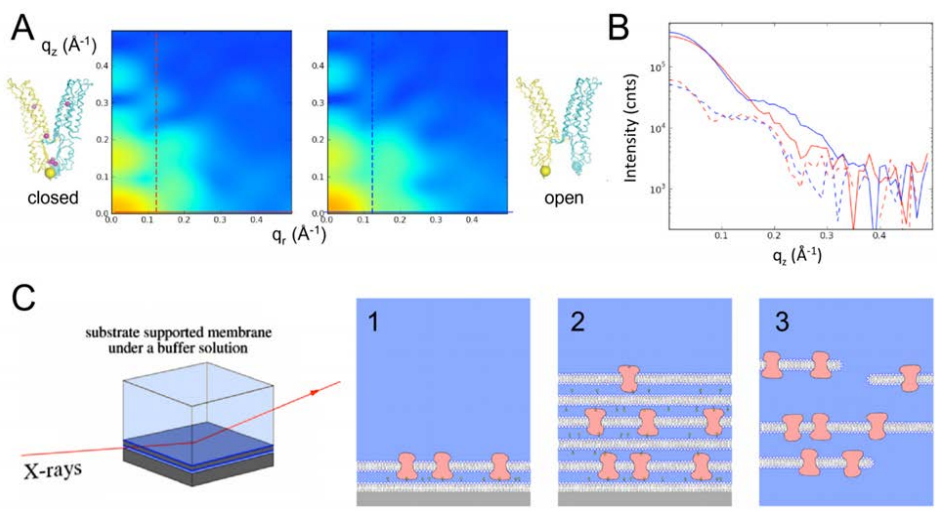

Figure 3. Feasibility of x-ray scattering studies of YiiP in planar lipid membranes. (A) The calculated form factor of the closed and open conformations of YiiP show qualitative differences. (B) These difference should be detectable as shown in line profiles corresponding to q_r=0.12 Å^{-1} (dashed lines) and q_z=0 (solid lines). Note that statistical noise has been added to simulate the scattered x-ray intensity from a single bilayer based on the beamline design described in section B. (C) Possible implementation of the x-ray scattering measurements in grazing incidence geometry. The sample could be prepared as (1) supported single bilayer, (2) supported multiple bilayers, and (3) magnetically aligned bicelles.

YiiP is a membrane transporter that catalyzes Zn^{2+}/H^{+} exchange across the inner membrane of *Escherichia coli*. Mammalian homologs of YiiP play critical roles in zinc homeostasis and cell signaling. Defective zinc transporters have been linked to, and are major drug targets for, diabetes and Alzheimer's disease. YiiP with its Y-shaped architecture dramatically differs from most cylindrically shaped membrane proteins. The incorporation of YiiP into the membrane necessitates the reorganization of lipids surrounding the irregular trans-membrane domain surface, to minimize hydrophobic mismatch. The ensuing bilayer deformation would directly impact the active site for zinc transport, which is characterized by a ~10 Å x 15 Å window open laterally to the lipid outer leaflet. The molecular responses to hydrophobic mismatch may have great functional significance. Emerging evidence suggests that a large collection of lipophilic channel modulators act by deforming the bilayer, and directly binding to the protein–lipid interface. X-ray scattering data from YiiP in planar lipid membranes can potentially reveal how the protein conformation depends on the presence of zinc ions. More importantly, due to the sensitivity of the scattering data to deformation in the lipid membrane structure, modeling of the scattering data may reveal the YiiP protein-lipid interface to help elucidate how lipids may reshape the active site for zinc transport.

2.2 Technical Requirements

Membrane proteins can be measured using grazing incidence x-ray scattering in single or multiple bilayers supported by a solid substrate (**Figure 3**C). Similar measurements on tobacco mosaic viruses adsorbed to a supported lipid monolayer have recently been demonstrated[25]. Such membrane structures need to be maintained under a bulk aqueous solution that defines the chemical environment surrounding the membrane proteins. Due to the low electron density contrast of the proteins against the lipid bilayer structure, background scattering from the bulk liquid will be a significant concern. This scattering background can be reduced by utilizing x-ray beams with a small vertical size to maximize the ratio between the volumes of the membrane structure and that of the surrounding bulk solvent within the x-ray beam. The line profiles plotted in **Figure 3**B correspond to a single layer of membrane structure, as probed by a beam 1 μm tall (in the direction of membrane normal). Solid state nuclear magnetic resonance (NMR) studies have employed magnetically aligned bicelles. These model membranes can also be utilized in x-ray scattering measurements. Note that similar studies have been reported using Langmuir lipid monolayers at a liquid–air interface[26]. The approach proposed here is expected to consume many fewer proteins. More importantly, substrate-supported samples can be frozen in vitrified ice—for instance by utilizing "slam" freezing[27], a technique widely used in electron microscopy of tissues—and measured at cryogenic temperatures to mitigate the adverse effect of radiation damage. For these measurements, x-ray energies of 16–20 keV will be needed to provide sufficient transmission though the bulk liquid.

To determine the structure of the lipid membranes that participate in biological processes, substrate-supported multiple-layered model membranes are often used. X-ray diffraction studies have successfully resolved the structures of the membrane stalk that occurs in membrane fusion[28] and the lipidic trans-membrane pores formed by small pore forming peptides[29,30] (**Figure 4**). These peptides usually have simple α-helical or β-hairpin structures. Collectively, they form pores in lipid membranes[31]. Structural determination of the pores has been achieved by coaxing the pores into a periodic lattice by manipulating the sample temperature and water content.

The electron density of the pore structure in membranes containing bromine (Br)-labeled lipids is then calculated from the diffraction data using multi-wavelength anomalous dispersion (MAD) phasing near the K absorption edge of Br [29,30]. The pore structures can also be studied even without the periodic lattice structure, as shown by neutron scattering[32]. This approach may be extended to pore-forming proteins including the apoptosis regulator BCL2 family of proteins, and bacterial toxins such as diphtheria toxin and colicins. For instance, the BCL2 protein Bax is

known to bind to the outer membranes of mitochondria and by a still unknown mechanism to form pores to release cytochrome C, which then triggers apoptosis.

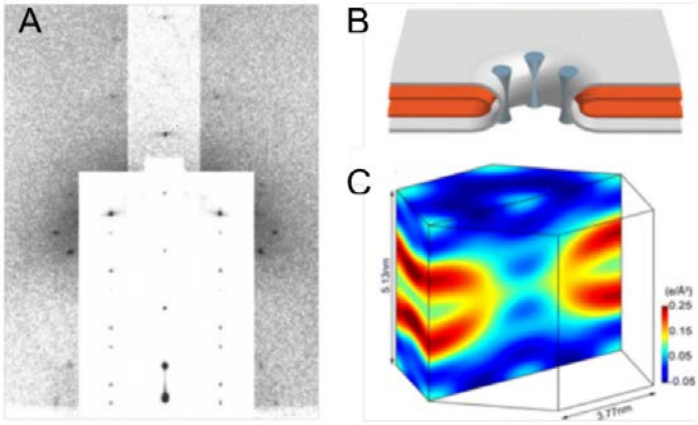

Figure 4. An example of diffraction from multi-layered lipid membrane structures. (A) Diffraction data from crystallized pores formed by a Bax-derived peptide. The electron density map of Br atoms in (C) derived from the data and MAD phasing confirms the hypothesized toroidal pore model (B). The location of the Br atoms is indicated by the orange-colored sheets in the model.

The electron density of the pore structure in membranes containing bromine (Br)-labeled lipids is then calculated from the diffraction data using multi-wavelength anomalous dispersion (MAD) phasing near the K absorption edge of Br[29,30]. The pore structures can also be studied even without the periodic lattice structure, as shown by neutron scattering[32]. This approach may be extended to pore-forming proteins including the apoptosis regulator BCL2 family of proteins, and bacterial toxins such as diphtheria toxin and colicins. For instance, the BCL2 protein Bax is known to bind to the outer membranes of mitochondria and by a still unknown mechanism to form pores to release cytochrome C, which then triggers apoptosis.

Recent studies have shown that the pore-forming properties of many of these proteins are similar to those of antimicrobial peptides [33–36]. Studying the pore-forming fragments of these proteins in model membranes therefore may help to elucidate how these proteins function. Grazing incidence x-ray scattering measurements on membranes should cover the *q*-range of ~0.006–2.0 $Å^{-1}$, so as to capture information on the proteins as well as the lipid chains within the membranes. The wide tuning range of the undulator planned for LIX also allows access to the K absorption edge of phosphorous (2.145 keV), a natural constituent of phospholipids, thereby eliminating the need to use labeled lipids to measure trans-membrane pores. Measurements will be conducted in a humidified helium environment with the detector fairly close to the sample, to capture the scattering data over the required *q* range.

3 X-ray Scattering-Based Scanning-Probe Imaging of Biological Tissues

3.1 Scientific Motivation

Biological tissues exhibit hierarchical structures, organized on multiple levels from the molecular to macroscopic scales. X-ray scattering using micron-sized beam spots allows for measurements to probe molecular and supramolecular organization underlying structural features observable in optical microscopy. Used as a scanning probe microscope, micro-beam x-ray scattering can be used to directly supply structural information complementary to other forms of microscopy that provide chemical information, such as IR or x-ray fluorescence.

One research area that will benefit from x-ray scattering-based scanning probe imaging is the relationship between the structure of bone and bone health. The characteristics of bone that influence its resistance to fracture have been loosely defined as bone quality [37]. However, there is no established method for comprehensively assessing bone quality. The gold standard for clinical assessment of bone strength is dual x-ray absorptiometry (DXA). DXA actually measures bone mineral density (BMD), which does not predictively define fracture risk. For example, teenagers

have essentially the same BMD as the elderly, but teens are not considered osteoporotic, and certainly are at little risk of fracture even given the greater physical demands they place on their skeleton. Instead, bone quality is greatly influenced by macroscopic, morphologic features such as a bone's cross-sectional cortical geometry[38], trabecular connectivity, the architecture of the trabeculae themselves[39], and the microscopic material structures.

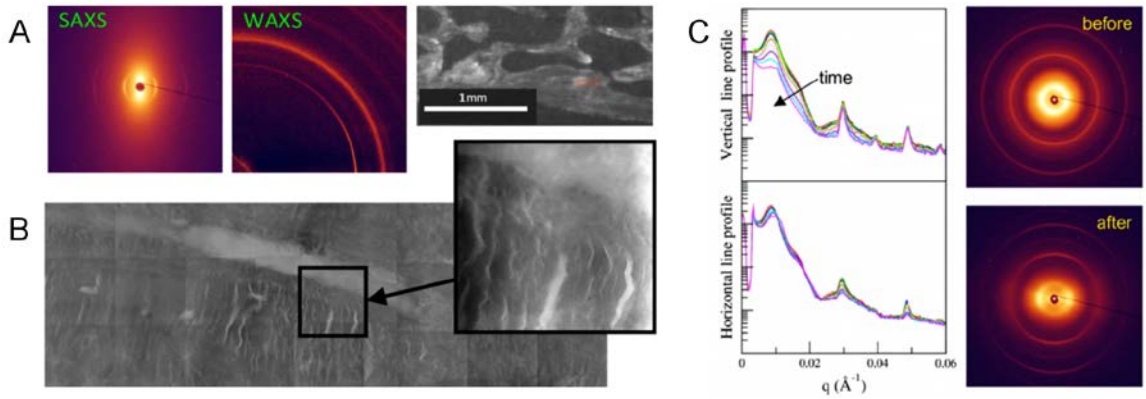

Figure 5. Examples of x-ray scattering from biological tissues. (A) X-ray scattering data collected from a 5 μm bone section at beamline X9 of NSLS. The x-ray spot size is ~200 μm x 60 μm (shown as the faint red box ~centered in the right half of the rightmost image of (A). The SAXS pattern reveals the amount, orientation, and order of the collagenous structure, whereas the WAXS signal indicates mineral species and density. Similar measurements can be performed at the proposed LIX beamline using 1 μm x-ray spot size, on structures such as hairline fracture in bone. (B) TXM image of a 5 μm bone section showing a 100 μm-long microdamage crack and hairline fractures oriented perpendicular to the crack. The field of view for the black outlined square is 32 μm. (C) Data collected at X9 show the preferential enzymatic degradation of collagen under load. The load is applied in the vertical direction. The diffraction peaks that correspond to the collagen *d* period are preserved in the vertical direction, while the scattering peak that corresponds to the inter-fibril spacing persists in the horizontal direction. The 2D images are collected before exposure to enzymes and after exposure of 110 minutes. With smaller x-ray beams, the same type of measurement could be performed on single fibers.

SAXS and wide-angle x-ray scattering (WAXS, see the example in **Figure 5**A) will provide critical information toward quantifying the role that collagen fibril diameter and orientation, as well as mineral crystal size and orientation, play in determining bone's mechanical behavior. More specifically, scanning probe x-ray scattering with ~1 μm spot size will be very useful for studying microdamage (**Figure 5**B). Microdamage in bone tissue occurs naturally as a result of loading on the body from normal activities. Although normal bone remodeling repairs these microdamage cracks, the anti-resorptive mechanism of certain drug treatments may slow bone remodeling and negatively affect the repair of microdamaged bone. Research on the chemical makeup of microdamage cracks and their mechanical properties, and thus their contribution to fracture risk, has started to emerge. For instance, FTIR (Fourier Transform Infrared) imaging has shown[40] that carbonate content and the collagen cross-linking structure were significantly altered in microdamaged bone, although it was not determined if this was the result of a microdamage crack or was present before the crack occurred. Micro-beam x-ray scattering can provide complimentary information on the collagen and mineral structure at/near microdamage cracks. The application of external strain[41] to a thin section of bone and simultaneous analysis with SAXS/WAXS could allow for direct observation of microdamage crack and hairline fracture initiation and growth. This may give insight into the microscopic structural mechanisms underlying such microdamage and how different drug treatments affect these processes.

The capability to perform x-ray scattering and diffraction measurements using a micron-size beam will also advance the field of tissue engineering. One of the goals in this scientific field is to produce engineered materials that carry out the functions of natural tissues. X-ray can help to

elucidate how the microscopy structures of natural tissues enable their functions and whether the engineered materials possess such required microscopic structures to be functional. An example of the application of x-ray scattering in this field is the study of the structural organization and remodeling of collagen in native and engineered tissues. Collagen is the dominant structural protein in vertebrate animals and plays a role in numerous health-related problems that affect the U.S. population (i.e., osteoarthritis, intervertebral disc degeneration, osteoporosis, etc.). Preliminary studies by the Ruberti group of Northeastern University have illustrated the feasibility of using x-rays to monitor load sculpting (**Figure 5**C). This group has also recently found that polymerization of collagen produces mechanical strain and, conversely, mechanical strain enhances collagen polymerization. Micron-sized x-ray beams will permit detailed dynamical observation of collagen assembly, alignment, and organization in single fibers (10–100 μm diameter) during the strain-induced polymerization process, which is expected to be on the time scale of seconds and longer. For instance, a collagenous filament stretched between a deposition needle and a calibrated micropipette can be measured as polymerization takes place. The polymerization force causes the micropipette to deflect, giving a measure of the tensile strain.

3.2 Technical Requirements

Spatial resolution in scanning probe measurements is determined by the x-ray spot size on the specimen. Since structural information on length scales smaller than ~1 μm can be accessed in reciprocal space, we do not foresee high demand for sub-micron beam sizes. Frequently, 2D imaging is not sufficient to comprehensively characterize the structure of interest, and sample sectioning is not always an option, such as in the proposed in-situ measurement on the collagen fiber. In these cases, tomographic methods can be employed, as has been demonstrated in the literature for simple fiber structures[42,43]. To collect scattering data from both organic and inorganic components in biological tissues, the instrument should cover the q-range of ~0.003–3.0 $Å^{-1}$.

1. Bartlett, A. I. & Radford, S. E. An expanding arsenal of experimental methods yields an explosion of insights into protein folding mechanisms. *Nat Struct Mol Biol* **16,** 582–588 (2009).

2. Dill, K. A., Ozkan, S. B., Shell, M. S. & Weikl, T. R. The Protein Folding Problem. *Annu. Rev. Biophys.* **37,** 289–316 (2008).

3. Schaeffer, R. D., Fersht, A. & Daggett, V. Combining experiment and simulation in protein folding: closing the gap for small model systems. *Curr. Opin. Struct. Biol.* **18,** 4–9 (2008).

4. Chiti, F. & Dobson, C. M. Protein Misfolding, Functional Amyloid, and Huamn Disease. *Annu. Rev. Biochem.* **75,** 333–366 (2006).

5. Vestergaard, B. *et al.* A Helical Structural Nucleus Is the Primary Elongating Unit of Insulin Amyloid Fibrils. *PLoS Biol* **5,** e134 (2007).

6. Baures, P. W., Peterson, S. A. & Kelly, J. W. Discovering transthyretin amyloid fibril inhibitors by limited screening. *Bioorg. Med. Chem.* **6,** 1389–1401 (1998).

7. Ray, S. S., Nowak, R. J., Brown, R. H. & Lansbury, P. T. Small-molecule-mediated stabilization of familial amyotrophic lateral sclerosis-linked superoxide dismutase mutants against unfolding and aggregation. *Proc. Natl. Acad. Sci. U. S. A.* **102,** 3639–3644 (2005).

8. Garst, A. D. & Batey, R. T. A switch in time: Detailing the life of a riboswitch. *Biochim. Biophys. Acta BBA - Gene Regul. Mech.* **1789,** 584–591 (September).

9. Cruz, J. A. & Westhof, E. The Dynamic Landscapes of RNA Architecture. *Cell* **136,** 604–609 (2009).

10. Sarabu, R. & Grimsby, J. Targeting glucokinase activation for the treatment of type 2 diabetes--a status review. *Curr. Opin. Drug Discov. Devel.* **8,** 631–637 (2005).

11. Russell, R. *et al.* Rapid compaction during RNA folding. *Proc. Natl. Acad. Sci.* **99,** 4266 –4271 (2002).

12. Roder, H., Maki, K. & Cheng, H. Early Events in Protein Folding Explored by Rapid Mixing Methods. *Chem. Rev.* **106,** 1836–1861 (2006).

13. Pollack, L. & Doniach, S. in *Biophysical, Chemical, and Functional Probes of RNA Structure, Interactions and Folding: Part B* **Volume 469,** 253–268 (Academic Press, 2009).

14. Bilsel, O., Kayatekin, C., Wallace, L. A. & Matthews, C. R. A microchannel solution mixer for studying microsecond protein folding reactions. *Rev. Sci. Instrum.* **76,** 014302 (2005).

15. Wu, Y., Kondrashkina, E., Kayatekin, C., Matthews, C. R. & Bilsel, O. Microsecond acquisition of heterogeneous structure in the folding of a TIM barrel protein. *Proc. Natl. Acad. Sci.* **105,** 13367–13372 (2008).

16. Akiyama, S. *et al.* Conformational landscape of cytochrome c folding studied by microsecond-resolved small-angle x-ray scattering. *Proc. Natl. Acad. Sci. U. S. A.* **99,** 1329–1334 (2002).

17. Pollack, L. *et al.* Time Resolved Collapse of a Folding Protein Observed with Small Angle X-Ray Scattering. *Phys. Rev. Lett.* **86,** 4962 (2001).

18. Park, H. Y. *et al.* Achieving Uniform Mixing in a Microfluidic Device: Hydrodynamic Focusing Prior to Mixing. *Anal. Chem.* **78,** 4465–4473 (2006).

19. Schlatterer, J. C. *et al.* Hinge Stiffness Is a Barrier to RNA Folding. *J. Mol. Biol.* **379,** 859–870 (2008).

20. Baird, N. J. *et al.* Extended Structures in RNA Folding Intermediates Are Due to Nonnative Interactions Rather than Electrostatic Repulsion. *J. Mol. Biol.* **397,** 1298–1306 (2010).

21. Meisburger, S., Pabit, S., Li, L., Blose, J. & Pollack, L. In preparation.

22. Kwok, L. W. *et al.* Concordant Exploration of the Kinetics of RNA Folding from Global and Local Perspectives. *J. Mol. Biol.* **355,** 282–293 (2006).

23. Lu, M. & Fu, D. Structure of the Zinc Transporter YiiP. *Science* **317,** 1746–1748 (2007).

24. Lu, M., Chai, J. & Fu, D. Structural Basis for Auto-regulation of the Zinc Transporter YiiP. *Nat. Struct. Mol. Biol.* **16,** 1063–1067 (2009).

25. Yang, L. *et al.* Structure and interaction in 2D assemblies of tobacco mosaic viruses. *Soft Matter* **5,** 4951 (2009).

26. Miller, C. E., Majewski, J., Watkins, E. B., Weygand, M. & Kuhl, T. L. Part II: Diffraction from Two-Dimensional Cholera Toxin Crystals Bound to Their Receptors in a Lipid Monolayer. *Biophys. J.* **95,** 641–647 (2008).

27. Switkes, M. & Ruberti, J. W. Rapid cryofixation/freeze fracture for the study of nanobubbles at solid–liquid interfaces. *Appl. Phys. Lett.* **84,** 4759 (2004).

28. Yang, L. & Huang, H. W. Observation of a Membrane Fusion Intermediate Structure. *Science* **297,** 1877–1879 (2002).

29. Qian, S., Wang, W., Yang, L. & Huang, H. W. Structure of the Alamethicin Pore Reconstructed by X-Ray Diffraction Analysis. *Biophys. J.* **94,** 3512–3522 (2008).

30. Qian, S., Wang, W., Yang, L. & Huang, H. W. Structure of transmembrane pore induced by Bax-derived peptide: Evidence for lipidic pores. *Proc. Natl. Acad. Sci.* **105,** 17379–17383 (2008).

31. Huang, H. W. Action of antimicrobial peptides: two-state model. *Biochemistry (Mosc.)* **39,** 8347–52 (2000).

32. Yang, L., Weiss, T. M., Harroun, T. A., Heller, W. T. & Huang, H. W. Supramolecular Structures of Peptide Assemblies in Membranes by Neutron Off-Plane Scattering: Method of Analysis. *Biophys J* **77,** 2648–2656 (1999).

33. Menestrina, G., Serra, M. D. & Lazarovici, P. *Pore-forming peptides and protein toxins*. (CRC Press, 2003).

34. Zakharov, S. D., Kotova, E. A., Antonenko, Y. N. & Cramer, W. A. On the role of lipid in colicin pore formation. *Biochim. Biophys. Acta BBA - Biomembr.* **1666,** 239–249 (2004).

35. Terrones, O. *et al.* Lipidic Pore Formation by the Concerted Action of Proapoptotic BAX and tBID. *J. Biol. Chem.* **279,** 30081–30091 (2004).

36. Basañez, G. *et al.* Bax-type Apoptotic Proteins Porate Pure Lipid Bilayers through a Mechanism Sensitive to Intrinsic Monolayer Curvature. *J. Biol. Chem.* **277,** 49360–49365 (2002).

37. Sievänen, H., Kannus, P. & Järvinen, T. L. N. Bone Quality: An Empty Term. *PLoS Med* **4,** e27 (2007).

38. Jepsen, K. J., Akkus, O. J., Majeska, R. J. & Nadeau, J. H. Hierarchical relationship between bone traits and mechanical properties in inbred mice. *Mamm. Genome* **14,** 97–104 (2003).

39. Judex, S. *et al.* Adaptations of Trabecular Bone to Low Magnitude Vibrations Result in More Uniform Stress and Strain Under Load. *Ann. Biomed. Eng.* **31,** 12–20 (2003).

40. Ruppel, M., Burr, D. & Miller, L. Chemical makeup of microdamaged bone differs from undamaged bone. *Bone* **39,** 318–324 (2006).

41. Gupta, H. S. *et al.* Cooperative deformation of mineral and collagen in bone at the nanoscale. *Proc. Natl. Acad. Sci. U. S. A.* **103,** 17741–17746 (2006).

42. Schroer, C. G. *et al.* Mapping the local nanostructure inside a specimen by tomographic small-angle x-ray scattering. *Appl. Phys. Lett.* **88,** 164102 (2006).

43. Kraft, P. *et al.* One-dimensional small-angle X-ray scattering tomography of dip-coated polyamide 6 monofilaments. *J. Synchrotron Radiat.* **17,** 257–262 (2010).